Climate Services xxx (xxxx) xxx–xxx

Contents lists available at ScienceDirect

Climate Services

journal homepage: www.elsevier.com/locate/cliser

Original research article

Sensitivity of large dengue epidemics in Ecuador to long-lead predictions of El Niño

Desislava Petrova[a,b,*,1], Rachel Lowe[a,b,c,d,1], Anna Stewart-Ibarra[e], Joan Ballester[a,b], Siem Jan Koopman[f], Xavier Rodó[a,b,g]

[a] Climate and Health Programme (CLIMA), Barcelona Institute for Global Health (ISGLOBAL), Barcelona, Catalonia, Spain
[b] Catalan Institute for Climate Sciences (IC3), Barcelona, Catalonia, Spain
[c] Department of Infectious Disease Epidemiology, London School of Hygiene and Tropical Medicine, London, UK
[d] Centre for the Mathematical Modelling of Infectious Diseases, London School of Hygiene & Tropical Medicine, London, UK
[e] Institute for Global Health and Translational Science, SUNY Upstate Medical University, Syracuse, NY, USA
[f] Vrije Universiteit Amsterdam, Amsterdam, The Netherlands
[g] Institució Catalana de Recerca i Estudis Avancats (ICREA), Barcelona, Catalonia, Spain

A B S T R A C T

Long-lead forecasts of El Niño events are lacking despite their enormous societal and economic impacts. These climatic events lead to floods and droughts in many tropical regions, and damage agriculture and the economy in poor countries. Due to their impact on local climate, they can also affect human health by increasing the risk of vector-borne diseases, such as dengue fever. Physical processes at the origin of this complex coupled ocean-atmosphere phenomenon are just beginning to be better understood, with subsurface processes and stored heat as two of the main driving forces leading to the development of El Niño in a quasi-periodic manner. Taking advantage of this new knowledge, a statistical dynamic components model, using a state space approach and predictors relevant to the El Niño evolution, was specifically tailored to forecast warm events at lead times of about 2 years (well beyond the traditional spring barrier limit in El Niño predictability). This forecasting scheme provides skilful information on the amplitude of El Niño events, their duration, and the peak time of the sea surface temperature anomalies at a sufficient lead time as to efficiently serve preventive public health actions. The long-lead El Niño predictions were coupled to a statistical dengue model to estimate dengue cases during the 1998 and the 2010 epidemics in El Oro Province in Ecuador, where dengue is hyper-endemic. The dengue model correctly estimated these two largest dengue epidemics even at a 2-year simulation lead time. Thus, information is successfully passed from the El Niño forecast domain to the dengue estimation domain, and the long-lead El Niño predictions are shown to potentially anticipate the magnitude of dengue epidemics in the peak season. The results validate the sensitivity of large dengue epidemics in the region to the El Niño forecasts within the proposed model coupling set-up and imply a potential for increasing lead-time in dengue prediction. This coupled model framework and exploratory analysis, based on El Niño predictions, could be easily extended to other similarly transmitted diseases in tropical and subtropical countries, which are directly and severely affected by the large-scale temperature and precipitation teleconnections occurring before, during and after El Niño events.

Practical Implications

Throughout Latin America and the Caribbean dengue fever is the main cause of mosquito-borne febrile illness (Guzman et al., 2015). Climate has been shown to have a significant impact on mosquito dynamics and hence on the spread of mosquito-transmitted diseases. However, most countries have not yet developed dengue early warning systems that use climate information to help prepare and respond to epidemics of the disease. This study shows how long-lead predictions of El Niño events can be incorporated in a dengue epidemic model to estimate large dengue epidemics in the province of El Oro, Ecuador, where dengue is hyper-endemic. The likelihood of some El Niño events can be predicted up to 2 years in advance. Therefore, forecasts of these events could serve as a timely early precursor of dengue, which should be considered by local public health authorities in disease monitoring, vector control and information systems. Our main findings are directly relevant to the public health sector in the province of El Oro in southern coastal Ecuador, as well as other dengue endemic regions that are affected by El Niño events. This represents an important step forward towards the development of an early warning system for dengue epidemics in the region. The methods and results of this study advance the state-

* Corresponding author at: Carrer del Doctor Aiguader 88, Barcelona 08003, Catalonia, Spain.
E-mail address: desislava.petrova@isglobal.org (D. Petrova).
[1] These authors contributed equally.

https://doi.org/10.1016/j.cliser.2019.02.003

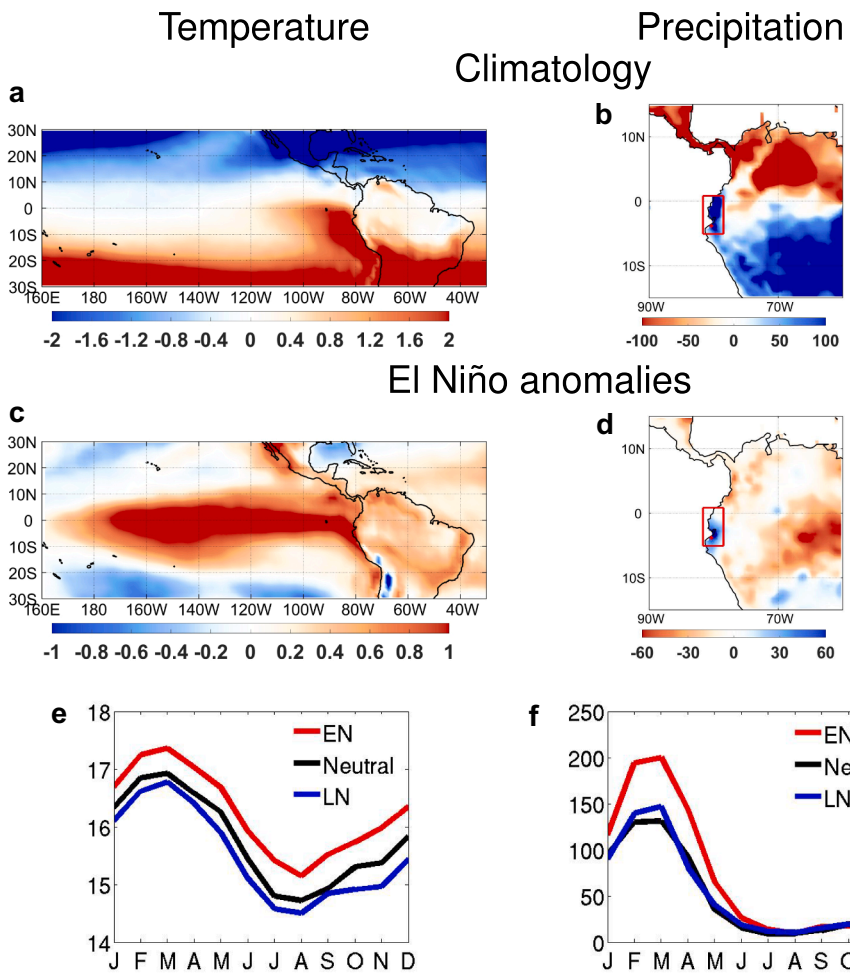

Fig. 1. Climate in El Oro Province, Ecuador. Minimum temperature (in [°C], shading) and precipitation (in [mm/month], shading) **a-b**, climatological values during the January-February-March season, and **c-d**, anomalous values during El Niño in January and February respectively, and **e-f**, average annual values during El Niño, La Niña and neutral years. The period used to calculate the climatology in panels a,b is 1981–2010. The EN events used for the calculation of composites are Dec. 1982, 1987, 1991, 1994, 1997, 2002, 2004, 2006, 2009 and the LN events are Dec. 1984, 1988, 1995, 1999, 2000, 2007, 2010, 2011. The data sets used are the NCEP/NCAR reanalysis for temperature and NOAA's PRECipitation REConstruction over Land for precipitation (Chen et al., 2002).

of-the-art in the area of climate services for health, by demonstrating the coupling of statistical models, to predict El Niño events and estimate dengue epidemics. This model framework could be deployed for other climate-sensitive diseases in regions directly affected by the El Niño Southern Oscillation. Vector-borne diseases, including dengue, are expanding globally, which has been attributed, in part, to climate change. Therefore, new strategies for combining climate and health methodologies are of high importance, particularly in resource-strained countries, where dengue early warning systems could be used for timely interventions to reduce the burden of disease as well as government spending on ineffective or unsustainable intervention activities.

1. Introduction

The El Niño Southern Oscillation (ENSO) is a major feature of tropical climate variability and triggers atmospheric teleconnections that directly impact the health (Diaz, 2000), resources and livelihoods of millions of people worldwide. Therefore, predicting individual ENSO events well in advance is of high relevance to decision makers in charge of planning and preparing for climate-related disasters. ENSO is a climate phenomenon characterized by coupled ocean-atmosphere anomalies in the tropical Pacific, commonly defined and assessed on the basis of sea surface temperature (SST) deviations in the Niño 3.4 region ([120–170°W, 5°S-5°N]), or by using the Oceanic Niño Index (ONI), which represents the three-month running-mean of SST anomalies in this region. El Niño (the warm phase) is defined by a positive ONI $\geqslant +0.5\,^{\circ}C$ for a period of at least 5 consecutive overlapping three-month seasons, while La Niña (the cold phase) by a negative ONI $\leqslant -0.5\,^{\circ}C$ for the same period of time (CPC, 2017). The abnormally high or low temperatures of the ocean affect the atmosphere directly above as a result of the strong ocean–atmosphere coupling in the tropical region (Bjerknes, 1969). This triggers atmospheric teleconnections that change the usual weather patterns globally (Ropelewski et al., 1987; Kiladis and Diaz, 1989; Rodó et al., 2006; Sarachik and Cane, 2010), especially in the vicinity of the equator. For example, in Ecuador the warm phase of the oscillation induces extreme events such as severe and prolonged flooding episodes that affect a sizeable portion of the population in the country (Larkin et al., 2002; Rossel et al., 2009; Recalde-Coronel et al., 2014).

Few studies exist on long-lead predictions of ENSO on the order of more than one year in advance (Chen et al., 2004; Ludescher et al., 2014; Gonzalez and Goddard, 2016). A recent study (Petrova et al., 2016), documented predictions of past El Niño events issued more than two years ahead of the peak SST anomalies, well before the first signs of the spring barrier in ENSO predictability. All the El Niño events that occurred in the period 1996–2015 were predicted at long lead times in retrospective forecasting mode. The forecasting scheme is based on structural time series modelling and analysis by state space methods (Durbin and Koopman, 2012). Additionally, predictors capturing the state of the atmosphere and ocean at different stages of the development of El Niño are incorporated so that specific variables such as wind stress, surface and subsurface ocean temperature are only used at their relative time of importance (see Petrova et al. (2016) for details). The long-lead capabilities of the model and the ENSO information that it provides – estimates of the timing, magnitude and duration of the

events – could be used as input in other climate and tropical disease prediction models, which could help to anticipate and assess the risk of climate-sensitive diseases for the countries and territories in the tropics, but also in other parts of the world where ENSO is known to have an impact.

The climate of Ecuador is heavily affected by inter-annual variability in ENSO. Due to its location along the equator, the country does not have well-distinguished seasons in regards to temperature, the mean ranges between 21° and 28 °C, with the highest values occurring during boreal winter (Fig. 1a shows the mean annual cycle averaged over the study period, but with the annual mean value removed, i.e. the average of the 12 monthly values of the mean annual cycle is equal to zero, which is here shown as the average over the months January-February-March). There is a marked wet season, which lasts from January to May (Bendix and Lauer, 1992; Moran-Tejeda et al., 2016) (Fig. 1b shows the same as Fig. 1a, but for precipitation), with rainfall highly related to the meridional movement of the Inter-Tropical Convergence Zone (ITCZ). When the ITCZ is in its southernmost position it brings warm and moist air to the coastal regions, resulting in increased precipitation rates and higher temperatures. Conversely, when the ITCZ is in its northernmost position, the coast is affected by upwelling processes in the equatorial Pacific, and by drier and cooler air masses (Rossel et al., 2009).

During El Niño strong convection triggered by warmer SST results in higher temperatures in southern coastal Ecuador (Aceituno, 1988; Bendix et al., 2006, Rossel et al., 2009, Moran-Tejeda et al., 2016) (Fig. 1ce), and much heavier precipitation (Fig. 1df) than observed during neutral or La Niña years (almost double the amount). Moreover, the peak of ENSO, which is normally at the end of the calendar year (between November-February), coincides with the beginning of the rainy season in Ecuador (Fig. 1b), and is immediately followed by the peak of precipitation anomalies associated with ENSO in southern Ecuador in February to March (Bendix et al., 2006) (Fig. 1df). Thus, the normal precipitation and temperature patterns in the area are significantly enhanced during El Niño. It has also been shown that the ENSO-associated SST anomalies and coastal precipitation are highly correlated (with correlation coefficients up to 0.8 for the Dec.-May period during El Niño (Coelho et al., 2002). For the province of El Oro we find a correlation of 0.5 for all months combined (Table 1). In addition, a positive relationship is found between El Niño and maximum and minimum temperature in the region (Moran-Tejeda et al., 2016), with a correlation of 0.7 (Table 1). ENSO also has predictive capacity for precipitation rates and temperature in the area (Rossel et al., 2009).

Several studies have shown that the El Niño cycle in certain areas is associated with changes in the risk of mosquito-transmitted diseases (Patz et al., 2002), such as malaria (Bouma et al., 2016), Rift Valley fever (Anyamba et al., 2009), dengue fever (Cazelles et al., 2005), and diseases caused by arboviruses other than dengue, including chikungunya (Chretien et al., 2007). Dengue fever is caused when the dengue virus (serotypes 1–4) is transmitted to people by the Aedes aegypti and Aedes albopictus mosquitoes. Dengue illness is characterized by fever and joint pain, causing a major burden, particularly in children (see WHO 2009 dengue guidelines or Stewart-Ibarra et al. (2018)). In a previous study (Stewart-Ibarra and Lowe, 2013), a statistical mixed model was developed to assess the importance of climatic and non-climatic drivers of dengue interannual variability in southern coastal Ecuador (in El Oro province). The authors found that the ONI, rainfall, and minimum temperature were positively associated with dengue (among other non-climate factors such as the DENV serotypes in circulation and the density of *Aedes aegypti*), with more cases of dengue expected during El Niño events (Fig. 2). Field studies in the same region also found that rainfall and minimum temperature were key drivers of *Aedes aegypti* dynamics (Stewart-Ibarra et al., 2013), providing mechanistic evidence for the influence of local climate on dengue transmission. Warmer temperatures increase the risk of dengue transmission up to an optimum temperature range of 26° to 29 °C (Mordecai et al., 2017), by increasing mosquito development rates, reproduction, survival, biting rates, and viral replication in the mosquito. Above this limit, transmission rates tend to decrease. Rainfall facilitates mosquito breeding by increasing the availability of larval habitat in abandoned rain-filled containers outdoors (Stewart-Ibarra et al., 2013). However, drought conditions that result in household water scarcity can also potentially increase larval habitat by increasing the number of water storage containers in and around the home (Lowe et al., 2018). Dengue transmission in El Oro has a well-defined seasonal pattern, and most cases are reported from February to May, which is the period of the year characterized by warmer and rainy weather (see Fig. 1ab and Fig. 1 in Stewart-Ibarra and Lowe (2013)).

In another more recent study (Lowe et al., 2017), the El Niño forecast from the dynamic components model and seasonal climate forecasts were used to predict in real time the evolution of the 2016 dengue season in the city of Machala, capital of El Oro Province, at a lead time up to 11 months, demonstrating that both the ENSO and the dengue model have operational predictive capacity. In this study, we build on these previous results by testing the sensitivity of dengue epidemic simulations to El Niño predictions of increasing lead time. More generally, the aim is to demonstrate the application of the long-lead ENSO predictions to estimate large dengue epidemics in an endemic region. We use forecasts of the 2009/10 El Niño event and the calculated ONI at multiple lead times, derived from the ENSO model, to produce simulated dengue probability distributions for El Oro province in southern coastal Ecuador for March 2010.

The 2010 dengue season was selected due to the exceptionally high burden of dengue in Ecuador and throughout Latin America and the Caribbean. In 2010, the province experienced the most severe dengue epidemic on record, with approximately 4008 suspected cases. People under 20 years of age bore the greatest burden of the disease (Stewart-Ibarra et al., 2014a). Statistical and wavelet analyses revealed that the epidemic may have been triggered by above normal minimum temperature and above normal rainfall during the 2009/10 El Niño event (Stewart-Ibarra and Lowe, 2013; Stewart-Ibarra et al., 2014b). Rainfall in February, preceding the peak of transmission, was almost double the long-term average (Fig. 2a). Social risk factors during the epidemic included household demographics (i.e., age and gender of heads of household) and housing conditions (i.e., access to piped water, poor housing construction) (Stewart-Ibarra et al., 2014b). Other regions also experienced major dengue epidemics in the same year, including Puerto Rico, which reported the largest historical epidemic (21,000 cases) (CDC, 2011). Globally, the greatest number of deaths due to dengue were reported in 2010, based on data from 1990 to 2013 (Stanaway et al., 2016).

The manuscript is structured as follows: Section 2 presents the results of the study. Section 2.1 shows the predictions of the 2009/10 El Niño event at increasing lead times up to 21 months, while Section 2.2 provides the respective dengue simulations using the dengue model

Table 1
Relationship between El Niño and local climate variables. Correlations between the Niño3.4 Index and the local climate variables (minimum temperature (in [°C]) and precipitation (in [mm/month]) in El Oro, Ecuador (mean anomalies) at the 90% significance level, (Niño3.4 Index leads the climate variables). The Niño3.4 Index is derived from the NOAA-OI-SST-V2 data set, provided by the NOAA/OAR/ESRL PSD (www.esrl.noaa.gov/psd/); minimum temperature and precipitation are derived from the Granja Santa Ines weather station located in Machala, Ecuador (3°17′26″ S, 79°54′5″ W, 5 m.a.s.l.).

Lead month	Niño3.4-Tmin	Niño3.4-precip.	Tmin-precip.
−3	0.57	0.29	0.28
−2	0.60	**0. 30**	0.34
−1	**0. 63**	0.29	**0. 42**
0	**0. 63**	0.29	**0. 42**

Values in bold are significant at the 90% significance level.

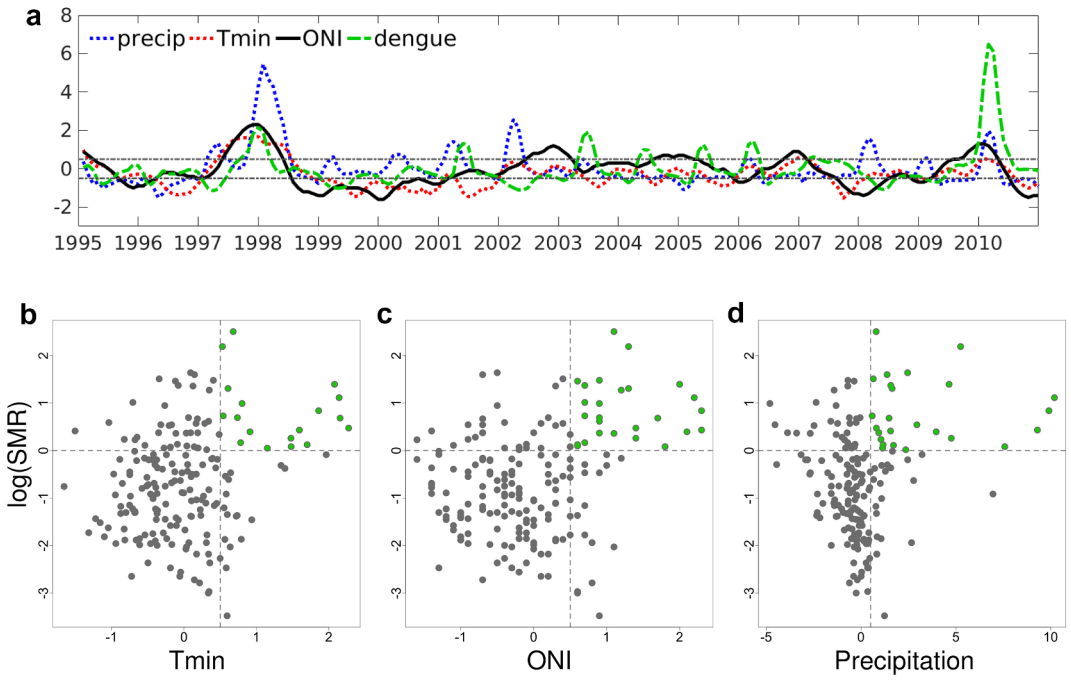

Fig. 2. Relationship between climate and dengue standardised morbidity ratios (SMR) in El Oro, Ecuador. **a**, Time series of the Oceanic Niño Index (solid black), minimum temperature (dotted red) and precipitation (dotted blue) from a grid point located in El Oro, and dengue SMR (dashed-dotted green) monthly anomalies. Dashed gray lines indicate the + /−0.5 (°C) threshold for El Niño and La Niña events. **b-d**, Scatter-plots of dengue SMR and minimum temperature monthly anomalies, the Oceanic Niño Index, and precipitation monthly anomalies. Green dots correspond to instances where Tmin, ONI and precipitation anomaly values > +0.5 and SMR > 1 (i.e. observed cases greater than expected cases). The ONI is derived from the NOAA-OI-SST-V2 data set, provided by the NOAA/OAR/ESRL PSD (www.esrl.noaa.gov/psd/); minimum temperature and precipitation are derived from the Granja Santa Ines weather station located in Machala, Ecuador (3°17′26″ S, 79°54′5″ W, 5 m.a.s.l.); dengue data is from the Ecuador Ministry of Health surveillance system.

with El Niño forecasts at different lead-time as predictors. In Sections 3 and 4 we interpret the results, discuss limitations and propose further work using a coupled El Niño-disease model framework. Section 5 provides details of the two modelling schemes that have been combined to produce the results.

2. Results

2.1. El Niño predictions

Fig. 3a shows predictions of the Niño3.4 region SST anomalies at lead times between 4 and 21 months prior to the peak of the 2009/10 El Niño together with the observed anomalies (black curve). The explanatory covariates used for forecasting are subsurface ocean temperature and zonal wind stress in the western and central tropical Pacific at their significant lag times (see Methods). A warm event is foreseen at all lead times, and as early as 21 months in advance (beige curve) the forecasting model already indicates a positive anomaly of approximately +1 °C for the peak month of December 2009. As the lead time decreases, forecasts and observations become more convergent, and the model prediction skill increases. An exception is the 8 month lead prediction (green curve), which is generally less accurate than the 12 month lead one. This is due to the spring barrier in ENSO prediction, which is characterized by the fact that forecasts for the end of the year initiated in the months March-May tend to be less accurate due to the presence of more noise in the atmosphere–ocean coupled system (Sarachik and Cane, 2010; Barnston et al., 2012). One full year before the peak of the El Niño (red curve), the forecast predicts the correct value of the warm peak in the Niño3.4 region of +1.46 °C at the correct time (December 2009; Table 2).

Depicted in Fig. 3b is the ONI for November-December-January (NDJ), calculated from the predictions in Fig. 3a. The 0 lead time corresponds to the observed values for the ONI at the end of 2009-beginning of 2010 (+1.3 °C for NDJ (CPC, 2017)). It is evident that the forecasting scheme is capable of providing highly accurate information about the amplitude of the event one year in advance of the mature phase of El Niño (magenta curve in Fig. 3b). Moreover, a medium-sized warm event (ONI≈ + 1 °C) is predicted for the eastern equatorial Pacific as early as 21 months ahead.

2.2. Dengue epidemics simulations

Observed and simulated dengue cases, using observed El Niño and local climate data, is shown in Fig. S1 for comparison with simulations driven by forecasts from the ENSO model, presented later in the article. The explanatory variables used to produce the dengue simulations included the House Index in the previous month (February 2010), anomalies of precipitation in the previous month (February 2010) and minimum temperature two months previous (January 2010), and the ONI for the NDJ period (i.e. a three month lag with respect to dengue cases). This combination of explanatory variables provides a predicative lead-time of one month.

In Fig. 4, the posterior probability distribution of dengue cases for March 2010 is simulated several times, varying the ONI value each time. In Fig. 4a, the observed NDJ ONI value is used to produce the dengue simulation (i.e. a dengue estimate providing a 3 month lead time). In Fig. 4b–f, predicted NDJ ONI values are used to simulate dengue, providing estimation lead times of 7, 11, 15, 20 and 24 months with respect to the March 2010 dengue peak. Climatological values of precipitation and temperature over previous years (i.e. climatology) and the House Index for the February prior to the forecast issue date were used at relevant time lags (see Methods). Following Bayesian methodology, we generate the posterior predictive distribution of the response by simulating new pseudo-observations using samples from the posterior distribution of the parameters in the model (Lowe et al., 2011). This allows for an additional layer of uncertainty in the response

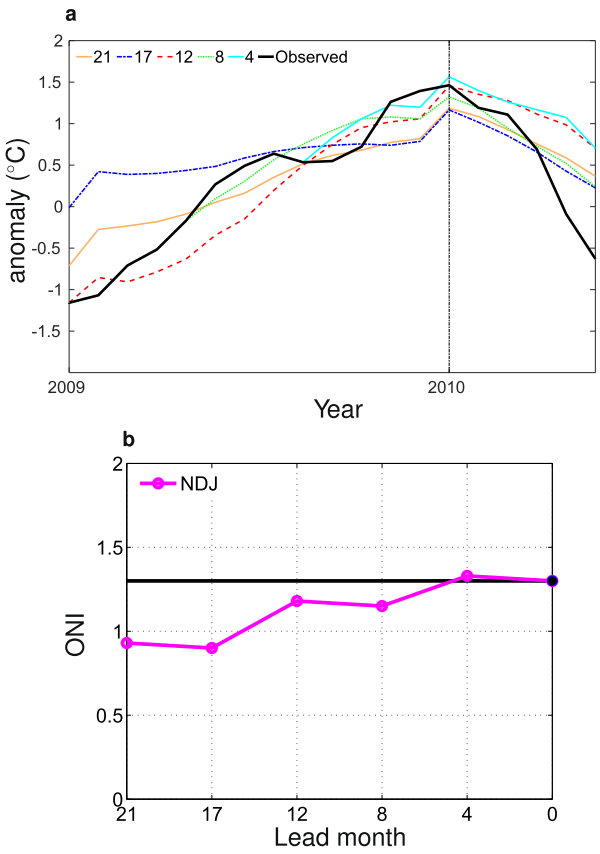

Fig. 3. Forecast of the 2009/10 El Niño event. **a**, Forecast of the Niño3.4 Index starting 21 (solid beige), 17 (dashed-dotted blue), 12 (dashed red), 8 (dotted green) and 4 (solid cyan) months ahead of the boreal winter peak. Observations are in solid black. The black dashed line indicates the peak of the observed anomaly. **b**, NDJ ONI (magenta) calculated from the forecasts started in the respective lead month before the peak of the 2009/10 El NiÑo. Lead month 0 corresponds to the observed value (black line and filled circle). The Niño3.4 Index is derived from the NOAA-OI-SST-V2 data set, provided by the NOAA/OAR/ESRL PSD (www.esrl.noaa.gov/psd/).

Table 2
Simulation of peak El Niño and dengue cases at different lead times. Modelled and observed El Niño peak anomalies in Dec. 2009 (in [°C]) and posterior mean dengue cases in March 2010. Lead month is with respect to the El Niño peak, and lead month in brackets is with respect to the dengue peak. The Niño3.4 Index is derived from the NOAA-OI-SST-V2 data set, provided by the NOAA/OAR/ESRL PSD (www.esrl.noaa.gov/psd/); dengue data is from the Ecuador Ministry of Health surveillance system.

Lead month	El Niño	Dengue
21 (24)	1.19	440
17 (20)	1.17	430
12 (15)	1.46	452
8 (11)	1.32	455
4 (7)	1.56	492
0 (3)	1.46	555
0 (0)	**1.46**	**979**

given the model parameters. Further information can be found in the Methods, Section 5.2, specifying the time period for which the model was fit (e.g. 2001–2010) and including more details about the model fitting procedure.

The dengue simulation in Fig. S1 provides a baseline reference for which to compare dengue simulations produced using forecasts of ONI from the ENSO model (see Fig. 4). Our focus is on analysing the sensitivity of the dengue simulations in Fig. 4 to the El Niño predictions as a function of lead time. The accuracy of the dengue probability estimations gradually decreases with increasing lead time (Table 2). However, even at 20 and 24 months, the posterior mean estimate is contained within the 95% credible intervals of the dengue probability distribution. Also, the estimation of 440 cases at 24 months lead time (Table 2) indicates an epidemic in dengue as compared to about 60 cases per year that are normally reported.

3. Discussion

The results described in the previous section demonstrate the high sensitivity of the large 2010 dengue epidemic in southern coastal Ecuador to information about the ONI from the ENSO forecasting model. ONI was previously found to be the key climate explanatory variable for dengue epidemics in this region (Stewart-Ibarra and Lowe, 2013). Moreover, it has a strong inter-annual signal, which makes it a good precursor. Also, considering that local minimum temperature and precipitation correlate with ONI (Table 1), the use of the climatological values of these variables in combination with the ONI forecast is shown to simulate the portion of the variability in dengue cases that is related to climate sufficiently well. Even at the longer simulation lead times of 20 and 24 months the dengue model accurately estimates a high chance of a dengue epidemic in March 2010 (Fig. 4f), and a sensitivity to the El Niño forecasts within the methodological framework is demonstrated. Therefore, the long-lead El Niño forecast information could be incorporated in a future early warning system for imminent epidemics in the region. The goal of this study was to perform a sensitivity analysis of the contribution of ONI forecasts as a predictor of large dengue epidemics with increasing lead times of up to two years. However, in practice, lead-times of one-year or less are used by public health-decision makers, who tend to plan vector-control activities within these shorter timeframes. Even a 3 month lead forecast using observed ONI values in a dengue prediction model would be of great value for planning vector control measures.

There are several limitations to this study and the results must be interpreted with caution. Here, we use a previously published exploratory dengue model (Stewart-Ibarra and Lowe, 2013) to simulate dengue estimates in 2010, replacing observed ONI values with forecast ONI values at progressively longer lead times. Future studies will develop more robust predictive dengue forecasting schemes (Lowe et al., 2017; Lowe et al., 2013; Lowe et al., 2014; Lowe et al., 2016) to produce out-of-sample predictions of dengue, to evaluate the feasibility of a real-time operational dengue early warning system up to two years ahead. However, the purpose of this study was to understand the extent to which ONI forecasts could extend predictive lead time, with other explanatory variables held constant. In a real-time prediction system, the ENSO signal will likely be obscured by other variables, such as mosquito abundance and knowledge of circulating serotypes, which are difficult to anticipate in advance.

Note that not all of the epidemics of dengue in El Oro are associated with El Niño events. Some dengue epidemics have occurred during non-El Niño years. Other factors not related to climate, such as the introduction of a new serotype or a lapse in vector control, could trigger a sizeable epidemic in the region. Additionally, the positive association between warm events and dengue in southern coastal Ecuador has been found only for the recent period since 1995, and in the cases of the 1997/98, 2002/03, 2004/05, 2006/07 and 2009/10 El Niño events in particular (Fig. 2a). For validation purposes, the same forecasts as for the 2009/10 El Niño and probability distributions for dengue were repeated for the prominent 1997/98 El Niño event and the second-largest epidemic in the observational record (Fig. 2a) that followed it (Figs. S2 and S3). As for the 2010 case, the dengue fitting and simulation was highly accurate at the 24 month lead time.

Finally, it should also be recognized that El Niño events are variable. For example, there are eastern Pacific canonical El Niño and central

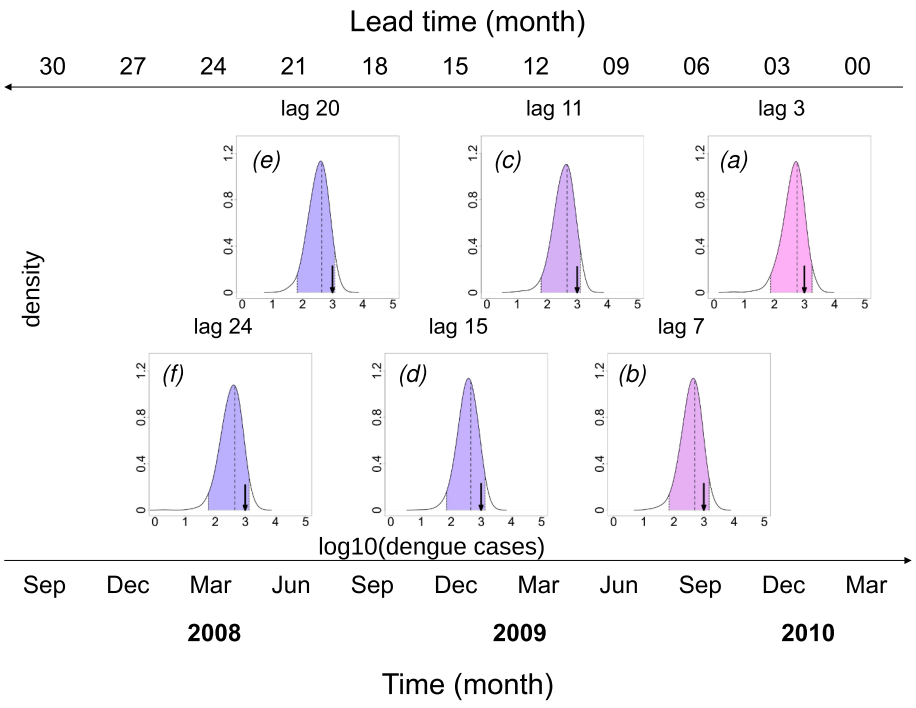

Fig. 4. Simulations of the 2010 dengue epidemic in El Oro, Ecuador. Posterior probability distribution of dengue cases (base-10 logarithmic scale) for March 2010 using **a**, observed ONI value for NDJ (3), and predicted ONI values for NDJ at lead times of **b**, 4 (7), **c**, 8 (11), **d**, 12 (15), **e**, 17 (20), and **f**, 21 (24) months with respect to the 2009/10 El Niño (with respect to the peak in dengue). All other explanatory variables are held constant. The mean of the simulated probability distribution (dashed line), 95% credible intervals (dotted lines) and observed dengue cases (arrow) are indicated. Dengue data is from the Ecuador Ministry of Health surveillance system.

Pacific "Modoki" El Niño (Ashok et al., 2007), and they could be associated with different teleconnections (Dewitte et al., 2012), and possible differences in the time lags that characterize them. For example, Ecuador is close to the eastern equatorial Pacific and thus promptly affected by the canonical events, but some climate change projections foresee more central Pacific ("Modoki" type) El Niño events in the future. The effect of El Niño on precipitation and temperature in Ecuador has been similar for the whole observational record, but it is not clear if this stable behaviour will be preserved with the changing climate (Tabachnick, 2010).

Moreover, different types of El Niño could be predicted with various rates of success (Barnston et al., 2012), and the smaller events are generally harder to predict. Thus, in an operational forecasting framework a false alarm for El Niño could also result in a false alarm for a dengue epidemic. Therefore, the credibility of the information provided to the end users could be limited by the predictability of the climate system, in this case represented by the metric of ONI. It is also possible that an epidemic could occur in a non-El Niño year, and one such epidemic actually happened in early 2006, which was a La Niña year. To prevent such false alarms in a future operational framework, the two models presented here should be recalibrated regularly, the forecast information should be updated frequently (as often as new information becomes available), and the level of uncertainty should be clearly communicated at each step.

4. Conclusion

Although the afore-mentioned issues are important and must be taken into consideration, a skilful ENSO forecasting scheme could provide highly valuable information and make possible the development of early warning systems for forthcoming disasters (Connor et al., 2008). In this study we demonstrated the ability of the ENSO forecasting model to predict a particular El Niño event and to deliver long-lead forecast information, which was then coupled to a partially climate-driven dengue exploratory scheme to assess the sensitivity of a dengue epidemic in El Oro in Ecuador in 2010. The ENSO model successfully predicted the 2009/10 El Niño at the very long lead time of 21 months, which provides a dengue simulation lead time of 24 months. Thus, we conclude that the long-lead El Niño forecasts may serve as potential very early precursors of large dengue epidemics in southern coastal Ecuador. The methodology could be optimized by considering El Niño-derived predictions of the local climate variables, especially of minimum temperature. The added value of such a potential long-lead prediction is mostly economic, as public funds for health, and in particular for epidemic prevention (vector control, community mobilization, purchasing of insecticides and laboratory diagnostic reagents), and vaccination campaigns (once a dengue vaccine becomes available), could be well planned and optimized. This example of successful coupling of an ENSO and a dengue model, and collaborative analysis between the spheres of climate science and infectious disease serves to demonstrate the potential benefit of climate predictors for increasing disease epidemic predictive lead time. Considering that dengue poses substantial strains to the health care systems in endemic tropical countries such as Ecuador, the results shown here contribute to the efforts for the development of an operational scientific tool to provide local decision makers with targeted health information, and to support and help them in planning their mitigation and adaptation measures.

5. Methods

5.1. ENSO forecasting model

A structural time series model (also referred to as a dynamic components model) adopted from (Petrova et al., 2016) has been used for the prediction of the 1997/98 and 2009/10 El Niño events. The model is built in terms of unobserved components – a trend, a seasonal, three cycle components, an irregular term and some explanatory regression variables. All components are subject to stochastic dynamic specifications that rely on error terms with mean zero and non-negative variances. The model is given by:

$$y_) = \mu_t + \gamma_t + \psi_{1t} + \psi_{2t} + \psi_{3t} + x_t'\delta + \varepsilon_t \quad (1)$$

where y_t represents the monthly Niño3.4 index at time t;μ_t is the trend component specified as a random walk process; γ_t is the seasonal component; ψ_{1t}, ψ_{2t} and ψ_{3t} are three cycles with different frequencies λ_j, ($j = 1, 2, 3$), persistences φ_{ψ_j} and variances $\sigma^2_{\kappa j}$; the term $x_t'\delta$ represents predictor regression variables; and ε_t represents the irregular term. The trend, seasonal, and cycle components are modeled as linear

dynamic stochastic functions of time (Harvey et al., 2000). More information about the components can be found in Durbin and Koopman (2012) and Harvey et al. (2000).

An important feature of the structural time series model is that it can be embedded in a state space framework (Durbin and Koopman, 2012), in which all unknown parameters associated with the model components are put in state and disturbance vectors, and estimated together in a dynamic way using the Kalman Filter (Kalman, 1960). Then forecasting is performed through signal extraction of the components. The software packages STAMP, SsfPack and OxMetrics (Koopman et al., 2008; Koopman et al., 2010; Doornik, 2013) are used for parameter estimation and forecasting.

The long-term variability in the mean of the Niño3.4 time series is incorporated in the model through the trend component. ENSO is also associated with a phase-locking to the annual cycle (Rasmusson et al., 1982; An et al., 2009), as its two phases usually peak in the Northern Hemisphere winter months of NDJ (Sarachik and Cane, 2010), and decay by the following summer. Thus, seasonality in the tropical Pacific is of prime importance for the timely growth and decline of ENSO (Tziperman et al., 1997; Krishnamurthy et al., 2015), and hence, for its accurate prediction. In our dynamic components model it is accounted for by the seasonal component. It has also been previously shown that other recurrent processes operating on inter-annual scales occur in the equatorial Pacific ocean and atmosphere that play a role in the development of the ENSO phenomenon (Jin et al., 2003; Rasmusson et al., 1990; Jiang et al., 1995). These variability modes have been found to have periods close to 1.5 years (near-annual mode), 2–2.5 years (quasi-biannual mode), and 4–6 years (quasi-quadrennial mode). They are included in the model in the form of stochastic cycle components. For more technical information regarding the model configuration and dynamical interpretation, the reader is referred to Petrova et al. (2016).

In addition to the components discussed above, a set of predictor regression variables are added to account for more specific dynamical variation occurring within the Niño3.4 region. These include surface and subsurface ocean temperature and wind stress in the equatorial western and central Pacific. The variables were selected on the basis of the dynamical processes in the equatorial Pacific seen to occur up to three years prior to the peak of an El Niño event (Petrova et al., 2016; Ballester et al., 2015).

ENSO is a mechanism through which, as a result of the prevailing easterly zonal winds, heat is accumulated in the western to central equatorial Pacific subsurface ocean, allowed to propagate to the eastern portion of the basin, and then released to the atmosphere or to higher latitudes after a saturation point is reached (Wyrtki, 1985; Zebiak, 1989; Jin, 1997). In this way, the zonal wind in the tropics directly affects the heat content of the ocean via Kelvin and Rossby downwelling and upwelling waves, which in turn influence SSTs (Ballester et al., 2015). The change in SSTs then affects the zonal wind patterns, and the so-called Bjerknes feedback between the ocean and the atmosphere is thus activated (Bjerknes, 1969). Considering these processes, we have selected regions in the tropical Pacific from which we obtain information about the coupled system in the form of time series, which are used as explanatory covariates in the ENSO forecasting model.

The structural time series ENSO model described above is capable of successfully predicting all the major El Niño events in the study period discussed here (see Fig. 9 in Petrova et al. (2016)). For the purposes of the current work it was applied to predict the extreme 1997/98 and the moderate-to-strong 2009/10 El Niño events at long lead times of 21 months. The aim was to use this early information to try to understand whether the prediction window for the anomalously high dengue epidemics known to have occurred in southern coastal Ecuador after these particular warm events (Stewart-Ibarra and Lowe, 2013) could theoretically be increased.

The data sets used for the predictions are the same as in Petrova et al. (2016). The climatology in Fig. 1a,b is calculated at every grid point by taking the mean annual cycle of Tmin and precipitation (i.e. the mean value for each calendar month averaged over the study period), but after removing the mean value of the whole time series (i.e. the average of the 12 values of the mean annual cycle is equal to zero). The El Niño-associated anomalies of Tmin and precipitation in Fig. 1c,d are calculated at each grid point by removing the mean annual cycle, and then compositing the anomalies only for El Niño years.

5.2. Dengue simulation model

Dengue is a mandatory notifiable disease in the province of El Oro, in southern coastal Ecuador, and cases include all suspected (clinically diagnosed) cases reported to the Ministry of Health surveillance system. Explanatory variables for the model used here include the ONI, local monthly rainfall and minimum temperature anomalies from the Granja Santa Ines weather station, operated by the National Institute of Meteorology and Hydrology of Ecuador and located in the city of Machala (3°17′26″ S, 79°54′5″ W, 5 m.a.s.l.) for the period 1995–2010, the mean monthly proportion of households with *Aedes aegypti* immatures (House Index) for the province of El Oro provided by the National Service for the Control of Vector-Borne Diseases, and the number of serotypes circulating in the country each month in the period 2001–2010. Serotypes are reported by the National Reference Center (NRC) for Dengue and other Arboviruses, the official diagnostic laboratory of the Ministry of Health. Temporally autocorrelated random effects for each calendar month were included to account for confounding factors, which might influence the annual cycle of dengue as well as climate, introducing an extra source of variability into the model. Yearly random effects were also included to capture non-climate related inter-annual variability, such as changes in vector control or reporting practices.

The statistical mixed model, described in Stewart-Ibarra and Lowe (2013), was used to simulate dengue cases in El Oro in March 2010. Briefly, a negative binomial generalised linear mixed model was formulated using monthly dengue cases data from January 2001 to December 2010 as the response variable and the expected number of cases, based on the underlying population, as the model offset (Lowe et al., 2011; Lowe et al., 2013). The model, comprising a combination of lagged climate variables, non-climate covariates and temporally structured and unstructured random effects, is formulated as follows:

$$y_t \sim NegBin(\mu_t, k) \tag{2}$$

$$log(\mu_t) = log(e_t) + \alpha + \beta_{t'(t)} + \sum \gamma_j x_{jt} + \delta_{T'(t)} + \sum \epsilon_j z_{jt} \tag{3}$$

where y_t is the monthly dengue cases, k is the overdispersion parameter, and μ_t is the mean dengue cases. Population effects were accounted for by including log of the expected cases e_t in the model as an offset at the linear predictor scale (which is assigned a coefficient of 1). The expected cases are calculated as the population at risk multiplied by the overall dengue detection rate (sum of all cases divided by the population summed over the time period) for El Oro. The model equation can then be rearranged such that the response is equivalent to the standardised morbidity ratio (SMR), defined as the ratio of observed to expected cases. The model then includes an intercept, α, temporally autocorrelated random effects for each calendar month, $\beta_{t'(t)}$, and exchangeable non-structured random effects for each year, $\delta_{T'(t)}$. The variables x_{jt} represent climate variables: anomalies of precipitation lagged by one month ($j = 1$), minimum temperature lagged by two months ($j = 2$), and the ONI index lagged by three months ($j = 3$). The variables z_{jt} represent non-climate factors: the House Index in the previous month (the proportion of homes with *Aedes aegypti* juveniles within a given period of time, as determined through routine vector surveillance by field technicians of the National Vector Service of the Ministry of Health of Ecuador), and the number of serotypes circulating in the country. Note, for the 1998 dengue estimation, we fitted a model to dengue data from January 1995 to December 2010. We used a model formulation similar to the one above but excluded the non-climate

factors term z_{jt}, as this data was not available prior to 2001 (see Stewart-Ibarra and Lowe, 2013).

The model parameters were estimated in a Bayesian framework using Markov Chain Monte Carlo methods (Gilks et al., 1996) (MCMC). This approach accounts for parameter uncertainty by assigning prior distributions to the parameters, with associated MCMC sampling yielding samples from the full posterior probability distribution of dengue in any given month. We then generated posterior predictive distributions of the response by simulating new pseudo-observations using samples from the posterior distribution of the parameters in the model (Lowe et al., 2011). This allows for an additional layer of uncertainty in the response given the model parameters.

The structured temporal random effects were assigned a first-order autoregressive month effect for each month ($t'(t) = 2, ...,12$) with month 1 (January) aliased to the model intercept, α, and subsequent months following a random walk or first difference prior in which each effect is derived from the immediately preceding effect. The temporally unstructured random year effects were assigned independent diffuse Gaussian exchangeable prior distributions.

The most significant variables associated with dengue variations were found to be the ONI lagged by three months, and the *Aedes aegypti* larval House Index in the previous month (Table S1). It was shown in Stewart-Ibarra and Lowe (2013) that a 1 °C increase in SST anomaly in Niño3.4 would result in 28% increase in dengue cases 3 months later, while 1% increase in the number of households with *Aedes aegypti* immatures would result in 48% increase in dengue cases one month later. Interestingly, ONI was found to be a more important climate variable than both Tmin and precipitation, which could imply that the impact of ENSO is not limited to these two variables. Finally, ENSO was shown to have a strong positive association with Tmin, while the association with precipitation was only weak (also see Table 1). In Fig. 2a we show that all El Niño events in the study period are related to positive anomalies in the minimum temperature. However, only the stronger El Niño events are clearly related to positive precipitation anomalies.

To generate the dengue epidemic simulations in this study, the observed ONI value used to estimate dengue cases in March 2010 was replaced by ONI predictions with lead times ranging from zero to 21 months. To understand the impact of increasing the lead-time of ONI forecasts, all other variables were held constant. For ONI forecasts 2–12 months, we used climatological values of precipitation (mean for February 2001–2009) and minimum temperature (mean for January 2001–2009) and the House Index for the previous year, February 2009. Note, for lead-times greater than 12 months, we recalculated the climatological averages for the years 2001–2008 and used the House Index for February 2008 (see schematic in Figure S4).

Author contributions

D.P. designed the study, carried out the ENSO forecasting experiments, analysed the data and wrote the manuscript. R.L. contributed to the design of the study and provided the dengue forecasts, A.S.I. provided the dengue data, J.B. provided the climate composites and all authors contributed to the development of ideas, the discussion and presentation of results and to the revision of the manuscript. The authors declare no competing financial interests.

Acknowledgement

The research leading to these results was supported by the DENFREE project (FP7-HEALTH.2011.2.3.3-2; 282378) and EUPORIAS project (FP7-ENV.2012.6.1-1; 308291), funded by the European Commission's Seventh Framework Research Programme. Many thanks to colleagues in Ecuador for providing the original data used in the analysis: Raul Mejia at the National Institute of Meteorology and Hydrology, Jhonny Real from the Ministry of Health of Ecuador, and Efrain Beltran and other colleagues from the National Vector Control Service (SNEM).

RL was supported by a Royal Society Dorothy Hodgkin Fellowship.

AMSI was additionally supported by NSF DEB EEID 1518681 and NSF DEB RAPID 1641145.

JB gratefully acknowledges funding from the European Union's Horizon 2020 research and innovation programme under grant agreements No 727852 (project Blue Action), 730004 (project PUCS), and 737480 (Marie Sklodowska-Curie fellowship ACCLIM). SJK acknowledges the support from CREATES (DNRF78) at Aarhus University, Denmark, funded by the Danish National Research Foundation. XR was in receipt of funds by the New Indigo project PARA-CLIM-CHANDIGARGH (Mineco, 2013).

The funding sources had no direct involvement in the conduct of the research and the preparation of the article.

Appendix A. Supplementary data

Supplementary data associated with this article can be found, in the online version, at https://doi.org/10.1016/j.cliser.2019.02.003.

References

Guzman, M.G., Harris, E., 2015. Dengue. Lancet 385 (9966), 453–465.
Diaz, H.F., 2000. El Niño and the Southern Oscillation: Multiscale Variability and Global and Regional Impacts. Cambridge University Press.
CPC, 2017. Cold and warm episodes by season. http://www.cpc.ncep.noaa.gov/products/analysis_monitoring/ensostuff/ensoyears.shtml.
Bjerknes, J., 1969. Atmospheric teleconnections from the equatorial Pacific. Mon. Weather Rev. 97, 163–172.
Ropelewski, C.F., Halpert, M.S., 1987. Global and regional scale precipitation patterns associated with El Niño/Southern Oscillation. Mon. Weather Rev. 115, 1606–1626.
Kiladis, G.N., Diaz, H.F., 1989. Global climatic anomalies associated with extremes in the Southern Oscillation. J. Clim. 2, 1069–1090.
Rodó, X., Rodriguez-Arias, M.A., Ballester, J., 2006. The role of ENSO in fostering teleconnection patterns between the tropical north Atlantic and the western Mediterranean basin. CLIVAR Exchanges 11, 26–27.
Sarachik, E., Cane, M., 2010. The El Niño Southern Oscillation Phenomenon. Cambridge University Press.
Larkin, N., Harrison, D., 2002. ENSO warm (El Niño) and cold (La Niña) event life cycles: ocean surface anomaly patterns, their symmetries, asymmetries, and implications. J. Clim. 15, 1118–1140.
Rossel, F., Cadier, E., 2009. El Niño and prediction of anomalous monthly rainfalls in Ecuador. Hydrol. Process. 23, 3253–3260.
Recalde-Coronel, C., Barnston, A.G., Muñoz, A.G., 2014. Predictability of December–April rainfall in coastal and Andean Ecuador. J. Appl. Meteorology Climatol. 53, 1471–1493.
Chen, D., Cane, M., Kaplan, A., Zebiak, S., Huang, D., 2004. Predictability of El Niño over the past 148 years. Nature 428, 15.
Ludescher, J., Gozolchiani, A., Bogachev, M.I., Bunde, A., Havlin, S., Schellnhuber, H.J., 2014. Very early warning of next El Niño. PNAS 111 (6), 2064–2066.
Gonzalez, P., Goddard, L., 2016. Long-lead ENSO predictability from CMIP5 decadal hindcasts. Clim. Dyn. 46, 3127–3147.
Petrova, D., Koopman, S.J., Ballester, J., Rodó, X., 2016. Improving the long-lead predictability of El Niño using a novel forecasting scheme based on a dynamic components model. Clim. Dyn.
Durbin, J., Koopman, S.J., 2012. Time Series Analysis by State Space Methods, second ed. Oxford University Press.
Bendix, J., Lauer, W., 1992. The rainy seasons in Ecuador and their climatic interpretation. Erdkunde 46, 118–134.
Moran-Tejeda, E., Bazo, J., Lopez-Moreno, J.I., Aguilar, E., Azorin-Molina, C., Sanchez-Lorenzo, A., Martinez, R., Nieto, J.J., Mejia, R., Martin-Hernandez, N., Vicente-Serrano, S.M., 2016. Climate trends and variability in Ecuador (1966–2011). Int. J. Climatol.
Aceituno, P., 1988. On the functioning of the Southern Oscillation in the South America sector Part I: Sufrace climate. Mon. Weather Rev. 116, 505–524.
Bendix, A., Bendix, J., 2006. Heavy rainfall episodes in Ecuador during El Niño events and associated regional atmospheric circulation and SST patterns. Adv. Geosci. 6, 43–49.
Coelho, C.A., Uvo, C.B., Ambrizzi, T., 2002. Exploring the impacts of the tropical Pacific SST on the precipitation patterns over South America during ENSO periods. Theoret. Appl. Climatol. 71, 185–197.
Patz, J.A., Kovats, R.S., 2002. Hotspots in climate change and human health. BMJ 325 (7372), 1094–1098.
Bouma, M.J., Siraj, A.S., Rodó, X., Pascual, M., 2016. El niño-based malaria epidemic warning for Oromia, Ethiopia, from august 2016 to July 2017. Trop. Med. Int. Health 21 (11), 1481–1488.
Anyamba, A., Chretien, J.-P., Small, J., Tucker, C.J., Formenty, P.B., Richardson, J.H., Britch, S.C., Schnabel, D.C., Erickson, R.L., Linthicum, K.J., 2009. Prediction of a rift valley fever outbreak. In: Proc. Nat. Acad. Sci. pages pnas-0806490106.

Cazelles, B., Chavez, M., McMichael, A.J., Hales, S., 2005. Nonstationary influence of El Niño on the synchronous dengue epidemics in Thailand. PLoS Med. 2 (4), e106.
Chretien, J.-P., Anyamba, A., Bedno, Sh.A., Breiman, R.F., Sang, R., Sergon, K., Powers, A.M., Onyango, C.O., Small, J., Tucker, C.J., et al., 2007. Drought-associated chikungunya emergence along coastal east Africa. Am. J. Trop. Med. Hyg. 76 (3), 405–407.
Stewart-Ibarra, A.M., Ryan, S.J., Kenneson, A., King, C.A., Abbott, M., Barbachano-Guerrero, A., Beltrn-Ayala, E., Borbor-Cordova, M.J., Crdenas, W.B., Cueva, C., Finkelstein, J.L., Lupone, C.D., Jarman, R.G., Maljkovic, B.I., Mehta, S., Polhemus, M., Silva, M., Endy, T.P., 2018. The burden of dengue fever and chikungunya in southern coastal Ecuador: Epidemiology, clinical presentation, and phylogenetics from the first two years of a prospective study. Am. J. Trop. Med. Hyg. 98, 1444–1459.
Stewart-Ibarra, A.M., Lowe, R., 2013. Climate and non-climate drivers of dengue epidemics in southern coastal Ecuador. Am. J. Trop. Med. Hyg. 88, 971–981.
Stewart-Ibarra, A.M., Ryan, S.J., Beltran, E., 2013. Dengue vector dynamics (Aedes aegypti) influenced by climate and social factors in Ecuador: implications for targeted control. PLOS ONE 8, 11.
Mordecai, E.A., Cohen, J.M., Evans, M.V., Gudapati, P., Johnson, L.R., Lippi, C.A., Miazgowicz, K., Murdock, C.C., Rohr, J.R., Ryan, S.J., et al., 2017. Detecting the impact of temperature on transmission of zika, dengue, and chikungunya using mechanistic models. PLoS Negl. Trop. Dis. 11 (4), e0005568.
Lowe, R., Gasparrini, A., Van Meerbeeck, C.J., Lippi, C.A., Mahon, R., Trotman, A.R., Rollock, L., Hinds, A.Q.J., Ryan, S.J., Stewart-Ibarra, A.M., 2018. Nonlinear and delayed impacts of climate on dengue risk in Barbados: a modelling study. PLoS Med. 15 (7), e1002613.
Lowe, R., Stewart-Ibarra, A.M., Petrova, D., García-Díez, M., Borbor-Cordova, M.J., Mejía, R., Regato, M., Rodó, X., 2017. Climate services for health: predicting the evolution of the 2016 dengue season in Machala, Ecuador. Lancet Planet. Health 1, e142–e151.
Stewart-Ibarra, A.M., Luzadis, V.A., Borbor-Cordova, M., et al., 2014a. A social-ecological analysis of community perceptions of dengue fever and Aedes aegypti in Machala, Ecuador. BMC Public Health pages, 1135.
Stewart-Ibarra, A.M., Muñoz, A.G., Ryan, S.J., et al., 2014b. Spatiotemporal clustering, climate periodicity, and social-ecological risk factors for dengue during an outbreak in Machala, Ecuador, in 2010. BMC Infect Dis. 14, 610.
CDC, 2011. Largest dengue outbreak in Puerto Rico history. CDC Dengue Update 2011; 3. http://www.cdc.gov/dengue/dengue_upd/resources/DengueUpdateVo3No1.pdf.
Stanaway, J.D., Shepard, D.S., Undurraga, E.A., et al., 2016. The global burden of dengue: an analysis from the Global Burden of Disease Study 2013. Lancet Infect. Dis.
Barnston, A., Tippett, M., L'Heureux, M., Li, Sh., DeWitt, D., 2012. Skill of real-time seasonal ENSO model predictions during 2002–11. Is our capability increasing? Am. Meteorol. Soc. 93, 631–651.
Lowe, R., Bailey, T.C., Stephenson, D.B., Graham, R.J., Coelho, C.A., Carvalho, M.Sá., Barcellos, C., 2011. Spatio-temporal modelling of climate-sensitive disease risk: Towards an early warning system for dengue in Brazil. Comput. Geosci. 37, 371–381.
Lowe, R., Bailey, T.C., Stephenson, D.B., Jupp, T.E., Graham, R.J., Barcellos, C., Carvalho, M.S., 2013. The development of an early warning system for climate-sensitive disease risk with a focus on dengue epidemics in Southeast Brazil. Stat. Med. 32, 864–883.
Lowe, R., Barcellos, Ch., Coelho, C.A.S., Bailey, T.C., Coelho, G.E., Graham, R., Jupp, T., Ramalho, W.M., Carvalho, M.Sá., Stephenson, D.B., et al., 2014. Dengue outlook for the world cup in Brazil: an early warning model framework driven by real-time seasonal climate forecasts. Lancet Infect. Dis. 14 (7), 619–626.
Lowe, R., Coelho, C.A.S., Barcellos, Ch., Carvalho, M.Sá., De Castro Catao, R., Coelho, G.E., Ramalho, W.M., Bailey, T.C., Stephenson, D.B., Rodó, X., 2016. Evaluating probabilistic dengue risk forecasts from a prototype early warning system for Brazil. Elife 5, e11285.
Ashok, K., Behera, S.K., Rao, S.A., Weng, H., Yamagata, T., 2007. El Niño Modoki and its possible teleconnection. J. Geophys. Res.: Oceans 112.
Dewitte, B., Vazquez-Cuervo, J., Goubanova, K., Illig, S., Takahashi, K., Cambon, G., Purca, S., Correa, D., Gutiérrez, D., Sifeddine, A., et al., 2012. Change in El Niño flavours over 1958–2008: Implications for the long-term trend of the upwelling off Peru. Deep Sea Res. Part II 77, 143–156.
Tabachnick, W.J., 2010. Challenges in predicting climate and environmental effects on vector-borne disease episystems in a changing world. J. Exp. Biol. 213, 946–954.
Connor, S.J., Mantilla, G.C., 2008. Seasonal Forecasts, Climatic Change and Human Health. Springer.
Harvey, A., Koopman, S.J., 2000. Signal extraction and the formulation of unobserved components models. Econ. J. 3, 84–107.
Kalman, R.E., 1960. A new approach to linear filtering and prediction problems. J. Basic Eng., Trans., ASMA, Series D 82, 35–45.
Koopman, S.J., Shephard, N., Doornik, J.A., 2008. Statistical Algorithms for Models in State Space Form: SsfPack 3.0. Timberlake Consultants Press, London.
Koopman, S.J., Harvey, A.C., Doornik, J.A., Shephard, N., 2010. Stamp 8.3: Structural Time Series Analyser, Modeller and Predictor. Timberlake Consultants, London.
Doornik, J.A., 2013. Object-Oriented Matrix Programming using Ox 7.0. Timberlake Consultants Ltd, London. Seehttp://www.doornik.com.
Rasmusson, E., Carpenter, T., 1982. Variations in tropical sea surface temperature and surface wind fields associated with the Southern Oscillation/El Niño. Mon. Weather Rev. 110, 354–384.
An, S.I., Choi, J., 2009. Seasonal locking of the ENSO asymmetry and its influence on the seasonal cycle of the tropical eastern Pacific sea surface temperature. Atmos. Res. 94, 3–9.
Tziperman, E., Zebiak, S., Cane, M., 1997. Mechanisms of seasonal – ENSO interaction. J. Atmos. Sci. 54, 61–71.
Krishnamurthy, L., Vecchi, G., Msadek, R., Wittenberg, A., Delworth, Th., Zeng, F., 2015. The seasonality of the great plains low-level jet and ENSO relationship. J. Clim. 28, 4525–4544.
Jin, F.F., Kug, J.S., An, S., Kang, I.S., 2003. A near-annual coupled ocean-atmosphere mode in the equatorial Pacific. Geophys. Res. Lett. 30.
Rasmusson, E., Wang, X., Ropelewski, Ch., 1990. The biennial component of ENSO variability. J. Mar. Syst. 1, 71–96.
Jiang, N., Neelin, D., Ghill, M., 1995. Quasi-quadrennial and quasi-biennial variability in the equatorial Pacific. J. Clim. Dyn. 12, 291–310.
Ballester, J., Bordoni, S., Petrova, D., Rodó, X., 2015. On the dynamical mechanism explaining the western pacific subsurface temperature buildup leading to ENSO events. Geophys. Res. Lett. 42, 2961–2967.
Wyrtki, K., 1985. Water displacements in the Pacific and the genesis of El Niño cycles. J. Geophys. Res. 90, 7129–7132.
Zebiak, S., 1989. Oceanic heat content variability and El Niño cycles. J. Phys. Oceanogr. 19, 475–486.
Jin, F.F., 1997. An equatorial ocean recharge paradigm for ENSO. Part I: conceptual model. J. Atmos. Sci. 54, 811–829.
Gilks, W.R., Richardson, S., Spiegelhalter, D.J., 1996. Markov Chain Monte Carlo in Practice. Chapman and Hall/CRC, Boca Raton, Florida, USA 486.
Chen, M., Xie, P., Janowiak, J.E., Arkin, P.A., 2002. Global land precipitation: a 50-yr monthly analysis based on gauge observations. J. Hydrometeorol. 3, 249–266.